

Photoreceptor evaluation after successful macular hole closure: an adaptive optics study

Ashish Markan, Rohan Chawla , Vinay Gupta, Manasi Tripathi, Anu Sharma and Atul Kumar

Ther Adv Ophthalmol

2019, Vol. 11: 1–7

DOI: 10.1177/
2515841419868132

© The Author(s), 2019.
Article reuse guidelines:
[sagepub.com/journals-](http://sagepub.com/journals-permissions)
[permissions](http://sagepub.com/journals-permissions)

Abstract

Objective: To study photoreceptor changes after a successful macular hole surgery using adaptive optics.

Materials and Methods: Three patients who underwent a successful macular hole surgery were studied. Cone density, spacing, and number of nearest neighbors were analyzed at 2° and 4° of eccentricity in all four quadrants using adaptive optics.

Results: All three patients gained a visual acuity better than logMAR 0.477 (Snellen equivalent 6/18) at 6 months following successful macular hole surgery. Following successful closure of the macular hole, photoreceptors were appreciated at 2° and 4° of eccentricity from the center. However, as compared with the fellow normal eye, cell density was reduced significantly in the inferior ($12,929.33 \pm 2047.50$ versus $23,839.67 \pm 3711.16$ cells/mm² at 2°) and temporal quadrant ($13,890 \pm 3424.26$ versus $22,578.67 \pm 5651.34$ cells/mm² at 2°), and intercell spacing was increased significantly in inferior (9.6 ± 0.92 versus 7.14 ± 0.545 μm) and nasal quadrant (8.83 ± 0.39 versus 7.49 ± 0.42 μm). Number of nearest neighbors was unaffected after the hole closure.

Conclusion: Postoperative recovery of vision after successful closure of the hole occurs because of the migration or shifting of cells from parafoveal retina toward the center. Cells nearest to the hole margin (at 2° eccentricity) appear to shift more as compared with cells which are further away.

Keywords: adaptive optics, cell density, macular hole, photoreceptor

Received: 28 May 2019; revised manuscript accepted: 15 July 2019.

Introduction

Macular hole is defined as a full-thickness defect of the neurosensory retina at the anatomical fovea. Management includes surgical intervention which involves pars plana vitrectomy with internal limiting membrane (ILM) peeling and intraocular gas tamponade.¹ Although surgical closure can be achieved in more than 90% of patients within few days, it can take up to 2 years for maximum visual recovery. In addition, the recovery is quite variable with persistence of relative scotomas and metamorphosia in some patients.^{2,3} A detailed and better understanding of the changes occurring at the cellular level post

macular hole surgery is required to understand the variability in visual recovery.

Optical coherence tomography (OCT) is an important noninvasive modality for diagnosing and confirming the closure of the hole in the post-operative period. Structural changes like integrity of inner segment–outer segment (IS–OS) junction and external limiting membrane (ELM) have been described to correlate with the visual acuity.^{4–7} OCT has a poor lateral resolution and is not able to provide sufficiently clear images of individual photoreceptor cells. Thus, it may not provide adequate insight into the causes of

Correspondence to:
Rohan Chawla
Assistant Professor, Dr.
Rajendra Prasad Centre
for Ophthalmic Sciences,
All India Institute of
Medical Sciences, New
Delhi 110029, India.
dr.rohanrpc@gmail.com

Ashish Markan
Vinay Gupta
Manasi Tripathi
Anu Sharma
Atul Kumar
Dr. Rajendra Prasad
Centre for Ophthalmic
Sciences, All India Institute
of Medical Sciences, New
Delhi, India

persistent visual disturbances in eyes with closed macular hole. The poor lateral resolution is because of the presence of optical aberrations, which can be overcome by use of adaptive optics (AO).

AO is a technology used to improve the performance of optical systems by reducing the effect of wavefront distortions. It measures the distortions in a wavefront and compensates for them with a device that corrects those errors, such as a deformable mirror or a liquid crystal array.^{8,9}

In this study, we used AO flood-illuminated technology (rtx1™; Imagine Eyes, Orsay, France) to study the cone density, spacing, and number of neighbors at 2° and 4° from the center after a successful hole closure.

Materials and methods

Three patients undergoing a successful macular hole surgery at our center were studied. The study was conducted in accordance with the tenets of the Declaration of Helsinki. Informed consent was obtained from all patients for publication of patient information and images for academic and research purpose.

All patients in this study underwent a comprehensive ophthalmologic examination at baseline and 6 months after surgical closure of macular hole. The following baseline parameters were assessed: best-corrected visual acuity (BCVA), assessed with the Snellen chart and expressed as the logarithm of the minimal angle of resolution (logMAR); intraocular pressure; and axial length, assessed using an IOL Master (Carl Zeiss Meditec, Dublin, CA, USA). At the baseline, we also performed a spectral-domain optical coherence tomography (SD-OCT; Zeiss Angioplex, Jena, Germany). At the 6-month postoperative evaluation, we measured BCVA and performed SD-OCT and AO imaging of the operated eye (rtx1, Imagine Eyes). AO was also performed in the fellow eye, and this was taken as a control.

Surgical steps

All three patients underwent 25-G pars plana vitrectomy. After performing core vitrectomy, triamcinolone was injected and posterior vitreous detachment was induced. Peripheral vitrectomy was completed. ILM was stained using 0.025% brilliant blue green (BBG) for 30 s. Inverted ILM

flap technique was performed followed by 20% SF6 tamponade. Patients were given strict prone position for 3 days. Macular hole was clinically closed at 1-week follow-up in all three patients.

Retinal imaging with the flood-illuminated AO retinal camera (rtx1)

We acquired on each eye a series of images of the retina using a commercially available flood-illuminated AO retinal camera (rtx1, Imagine Eyes).¹⁰ A set of 40 raw images of the same retinal area was acquired at a rate of 9.5 frames per second, with an exposure time of 10 ms to form the final image. The final AO image was averaged in a 4° × 4° field (i.e. 1500 pixels × 1500 pixels). Images were acquired at 2° and 4° of eccentricity along the four meridians (nasal, temporal, superior, and inferior). The subject was asked to fixate on a yellow cross controlled by the operator. The rtx1 is based on a Shack–Hartmann wavefront sensor (Haso3-32; Imagine Optic, Orsay, France) illuminated at 780 nm and a deformable mirror (mirao 52-e; Imagine Eyes). Cones are automatically detected by a software provided by the manufacturer (AOdetect Mosaic b13; Imagine Eyes). The background of the image is removed, and the histogram is stretched, then adaptive and multiple-scale digital filters are applied to the resulting image. The local maxima of the resulting filtered image were detected. Their spatial distribution was analyzed in terms of intercone spacing, local cell density, and number of nearest neighbors using Delaunay triangulation and Voronoi diagrams.^{11,12} Cone mosaic metrics (local density, spacing, and number of neighbors) were analyzed at 2° and 4°. Cones within the 2° central area (i.e. up to 1° from the center of the fovea) cannot be resolved because of the limit of resolution of the device.

Wilcoxon rank-sum (Mann–Whitney) test was used as a statistical method to compare cone mosaic metrics at various degrees of eccentricity in operated and fellow eyes.

Results

All three patients were analyzed at 6 months after the surgery. All the patients had type 1 closure on SD-OCT. All three patients had a postoperative BCVA better than logMAR 0.477 (equivalent to Snellen visual acuity of 6/18) at 6-month follow-up.

The mean cone density in superior quadrant was $15,716 \pm 283.92$ and $11,965 \pm 2985.63$ cells/mm²,

Table 1. Quadrantwise analysis of cell density in operated and fellow eyes.

Subject	D2s	D4s	D2i	D4i	D2t	D4t	D2n	D4n
Cell density (operated eye)								
1	15,397	14,268	10,573	11,225	14,355	12,525	17,438	14,067
2	15,810	13,036	14,275	18,827	10,257	10,890	18,969	14,740
3	15,941	8592	13,940	8628	17,058	13,600	15,809	16,126
Cell density (fellow eye)								
1	19,686	14,791	27,224	15,417	28,840	20,119	22,942	13,356
2	14,187	11,192	19,871	11,970	17,856	13,667	18,776	13,667
3	26,604	NC	24,424	NC	21,040	NC	23,333	NC

D2i, cell density at 2° inferior; D2n, cell density at 2° nasal; D2s, cell density at 2° superior; D2t, cell density at 2° temporal; D4i, cell density at 4° inferior; D4n, cell density at 4° nasal; D4s, cell density at 4° superior; D4t, cell density at 4° temporal; NC, not able to capture.

Cell density expressed as cells/mm².

in inferior quadrant was $12,929 \pm 2049.50$ and $12,893 \pm 5300.22$ cells/mm², in temporal quadrant was $13,890 \pm 3424.26$ and $12,338 \pm 1364$ cells/mm², and in nasal quadrant was $17,405 \pm 1580.25$ and $14,977 \pm 1049.87$ cells/mm² at 2° and 4° eccentricity, respectively. Spacing in superior quadrant was 8.72 ± 0.18 μ m and 10.09 ± 1.23 μ m, in inferior quadrant was 9.6 ± 1.51 μ m and 9.9 ± 1.5 μ m, in temporal quadrant was 9.28 ± 1.20 μ m and 0.52 ± 0.24 μ m, and in nasal quadrant was 8.83 ± 0.39 μ m and 8.82 ± 0.51 μ m at 2° and 4° eccentricity, respectively. On comparing with the control eyes, it was seen that cone density was significantly reduced in inferior and temporal quadrants at 2° ($p=0.04$ and 0.04 , respectively). Similarly, spacing between the cones was significantly increased at 2° in inferior and nasal quadrants ($p=0.049$ and 0.04 , respectively). At 4° also, the number was less than normal and the spacing was increased, but it did not reach statistical significance.

Based on Voronoi analysis, numbers of nearest neighbor cones were counted. It was seen that 87.23% and 83.73% in superior quadrant, 88.16% and 87.93% in temporal quadrant, 88.7% and 89.16% in nasal quadrant, and 85.16% and 86.9% in inferior quadrant had between five and seven neighbors at 2° and 4° of eccentricity, respectively. In comparison with the control eye, there was no difference in any of the quadrants, showing that arrangement of the cells is not significantly affected during closure of the macular hole.

Cone density, spacing, and number of nearest neighbors with five to seven neighbors of all three subjects are shown in Tables 1–3, respectively. In subject 3, analysis of the above parameters was not possible at 4° of eccentricity because of the poor image quality. Figure 1(a) and (b) shows AO imaging and Voronoi analysis done in patient 2 at 2° of eccentricity in temporal quadrant, respectively.

Preoperative and postoperative OCT images of patients 1, 2, and 3 are shown in Figure 2(a)–(f).

Table 4 shows detailed staging and characteristics of macular hole of all three patients.

Discussion

In this case series, we tried to evaluate the photoreceptor mosaic pattern after successful closure of macular hole on AO. This is, to our knowledge, first study evaluating photoreceptor density, spacing, and nearest neighbors on AO using flood-illuminated optics. Assessment was made after 6 months, which we believe is sufficient time period for structural remodeling of photoreceptor layers and stabilization of visual acuity. Our study showed that there was a reduction in cell density at 2° of eccentricity in all the quadrants, but it was in inferior and temporal quadrant that these values were significantly reduced. Even at 4° of eccentricity, there was reduction in cone density, though the values were not significant. Similarly,

Table 2. Quadrantwise spacing of cells in operated and fellow eyes.

Subject	S2s	S4s	S2i	S4i	S2t	S4t	S2n	S4n
Spacing (operated eye)								
1	8.75	9.48	9.2	8.36	10.53	9.61	9.21	9.01
2	8.9	9.29	10.66	9.98	9.2	9.72	8.42	9.21
3	8.53	11.51	8.94	11.38	8.13	9.25	8.86	8.24
Spacing (fellow eye)								
1	7.91	8.98	6.65	8.91	6.54	7.8	7.26	8.58
2	9.14	10.11	7.73	9.81	8.31	9.28	7.98	9.33
3	6.74	NC	7.06	NC	7.61	NC	7.24	NC

NC, not able to capture; S2i, spacing at 2° inferior; S2n, spacing at 2° nasal; S2s, spacing at 2° superior; S2t, spacing at 2° temporal; S4i, spacing at 4° inferior; S4n, spacing at 4° nasal; S4s, spacing at 4° superior; S4t, spacing at 4° temporal. Spacing expressed as μm .

Table 3. Quadrantwise analysis of number of nearest neighbors in operated and fellow eyes.

Subject	Nn2s	Nn4s	Nn2i	Nn4i	Nn2t	Nn4t	Nn2n	Nn4n
Number of nearest neighbors (operated eye)								
1	90.3	86.7	84.2	92.2	83	83.3	90.2	91.5
2	89.7	85.2	88	90.7	88.4	93.6	89.2	86
3	81.7	79.3	83.3	77.8	93.1	86.9	86.7	90
Number of nearest neighbors (fellow eye)								
1	91.6	98.2	93.2	91.2	93.6	100.1	87.3	93.9
2	82.1	83.3	94.9	90	89.8	96.3	85.7	79.3
3	99	NC	85.2	NC	92.6	NC	86.2	NC

NC, not able to capture; Nn2i, number of nearest neighbors at 2° inferior; Nn2n, number of nearest neighbors at 2° nasal; Nn2s, number of nearest neighbors at 2° superior; Nn2t, number of nearest neighbors at 2° temporal; Nn4i, number of nearest neighbors at 4° inferior; Nn4n, number of nearest neighbors at 4° nasal; Nn4s, number of nearest neighbors at 4° superior; Nn4t, number of nearest neighbors at 4° temporal. Number of nearest neighbors expressed as percentage.

spacing between the cones was increased in all the quadrants, significantly more in inferior and nasal quadrant at 2° of eccentricity. This reduction in cell density and increased spacing is suggestive of probable migration of the cells from the parafoveal retina toward the center of the hole. Previous studies have also shown decreased cell density on AO at 6-month follow-up, but have correlated decreased cell density to photoreceptor disruption and loss.¹³ This is contrary to what has been proposed by Gass¹⁴ during the pathogenesis of

hole formation. According to Gass, there is no photoreceptor loss during the hole formation, and the operculum tissue contains condensed hyaloid cortex. On the contrary, there are studies which have shown presence of photoreceptor elements in the operculum on immunocytochemical analysis.¹⁵ Our study shows that though the number of cells migrating toward the fovea does not reach the normal cell count, the number of nearest neighbors of these cells is similar to the normal pattern. This could indicate that

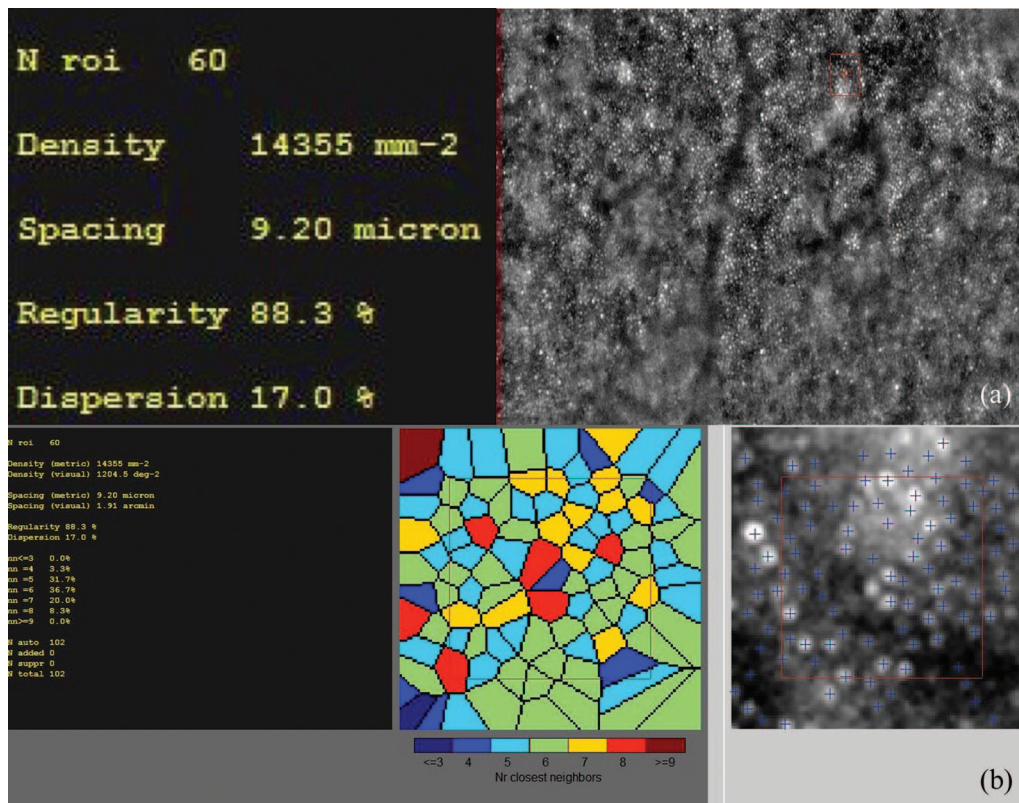


Figure 1. (a) Adaptive optics imaging using rtx1 in patient 2 with a surgically closed macular hole at 2° of eccentricity in temporal quadrant and (b) Voronoi analysis done in patient 2 after successful hole closure at 2° of eccentricity in temporal quadrant.

the redistribution of cells occurs to try and achieve a normal anatomical arrangement. This arrangement also has a correlation with the BCVA. All three of our patients had achieved a visual acuity better than logMAR 0.477. Patients 1 and 2 had a BCVA of logMAR 0.301 (Snellen equivalent of 6/18), and Patient 3 had a BCVA of logMAR 0.176 (Snellen equivalent of 6/12). Spacing and number of nearest neighbors were not evaluated by Ooto and colleagues in their study. On the contrary, the study by Hansen and colleagues has refuted cell migration by showing constant cell density and improvement in the cone mosaic pattern over serial AO.¹⁶ Improvement in mosaic pattern can be due to resolution of retinal edema and decreased tissue inflammation with time. Cell density was unchanged on serial AO imaging in this study. This could mean that cell migration ceases to happen after a particular time period. The cell migration could be a consequence of only a simple return in seat of photoreceptors that were displaced at the edge of the full-thickness macular hole (FTMH) or in addition there could be migration of the parafoveal photoreceptors

toward the center of the closed hole. It could also be a combination of both. It is not possible to establish the exact nature of migration/shift from this study. A limitation of our study is that we did not do a serial AO imaging. Another interesting finding from our study is that despite a low cell density, as compared with the other eye, our patients had a good gain of vision. Thus, the absolute cone count does not linearly correlate with visual acuity. Other factors such as cone arrangement and cone-midget bipolar and ganglion cell ratio/interaction also need to be studied. We were unable to assess the ganglion cells with the AO machine used by us.

Our study has several limitations. First, we had a small sample size. This is due to difficulties encountered while capturing the AO images using flood-illuminated optics. Practically, it is difficult to simultaneously focus both at the center of the hole and various degrees of eccentricity due to different scanning depths at these points. Obtaining a good quality image also requires good central fixation which is usually poor in

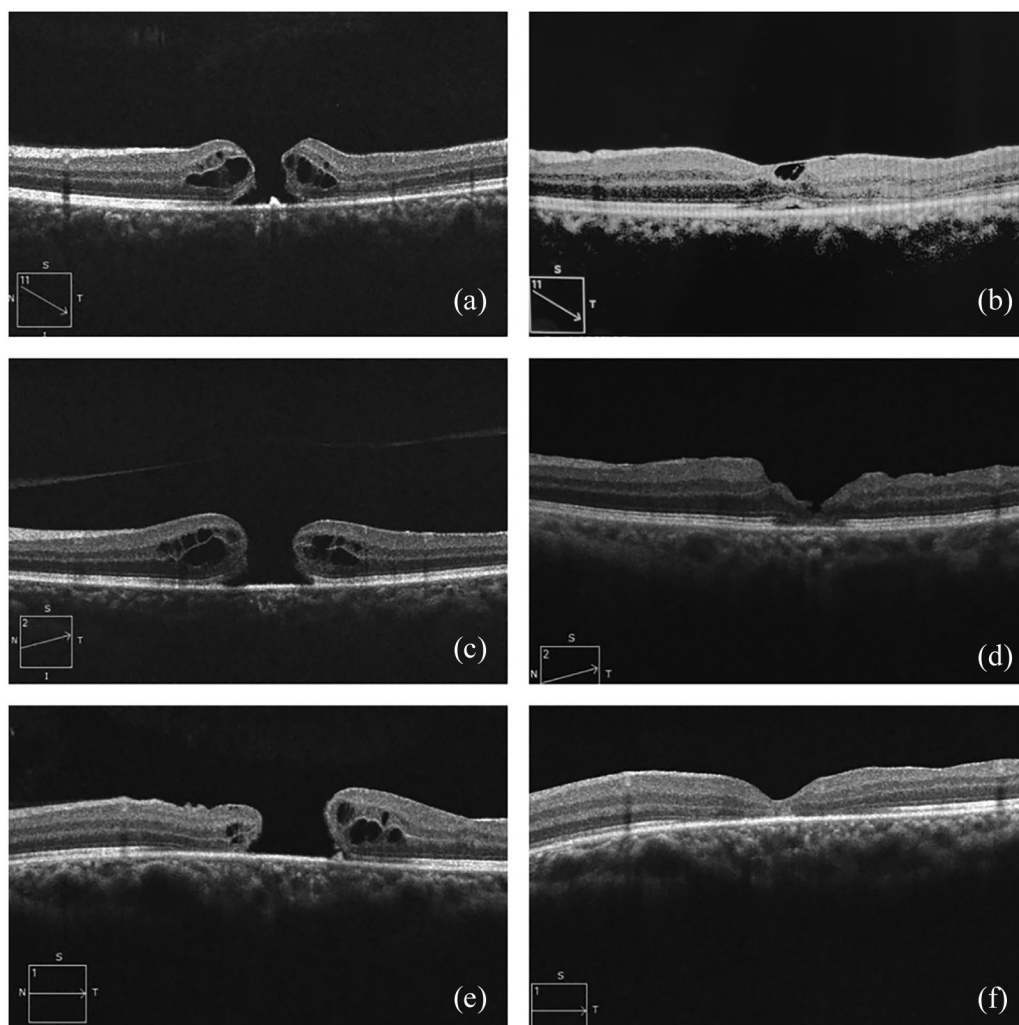


Figure 2. (a), (c), and (e) Pre-op OCT of macular hole in patients 1, 2, and 3, respectively. (b), (d), and (f) Post-op OCT showing type 1 closure in patients 1, 2, and 3, respectively. OCT, optical coherence tomography.

Table 4. Detailed staging and characteristics of macular hole of all three patients.

	Gass staging	IVMTS staging	Minimum diameter (μm)	Type of closure	Pre-op visual acuity	Post-op visual acuity
Patient 1	Stage 2	Stage 2	313	Type 1	4/60 (20/320)	6/18 (20/60)
Patient 2	Stage 4	Stage 4	515	Type 1	6/60 (20/100)	6/18 (20/60)
Patient 3	Stage 3	Stage 3	1068	Type 1	6/60 (20/100)	6/12 (20/40)

IVMTS, International Vitreomacular Traction Study.

patients with operated macular hole. Thus, we included only these three patients for whom we felt that the images were of adequate quality and the cell counts were fairly interpretable. The standard deviation of some of the counts obtained is high. But this is due to the imaging limitation of present-generation AO technology. Second, we

were unable to capture clearly individual cone photoreceptors in the foveal center. Third, AO imaging was not done preoperatively for these eyes, as again in the presence of a large central hole, it was not possible to capture good images. Last, serial AO imaging was not done, which can be helpful in better understanding of the

microstructural changes during closure of the macular hole.

To conclude, we believe that postoperative recovery of vision after successful closure of the hole occurs because of the migration or shifting of cells from parafoveal retina toward the center. It is the cells nearest to the hole margin (at 2° eccentricity) which shift the most as compared with cells which are further away. The numbers of cells and their arrangement both have a bearing on visual recovery. Further studies with a larger sample size, serial follow-up, and further enhanced AO imaging platforms would add more to our understanding of the correlation of anatomical restoration to visual gain.

Conflict of interest statement

The authors declared no potential conflicts of interest with respect to the research, authorship, and/or publication of this article.

Ethical approval

For the study, there was no change done to the medical/surgical treatment protocol of the patient. It is just an analysis of standard imaging data of the cases. Thus, ethical clearance was not applied for.

Funding

The authors received no financial support for the research, authorship, and/or publication of this article.

ORCID iD

Rohan Chawla  <https://orcid.org/0000-0002-6791-4435>

References

- Kelly NE and Wendel RT. Vitreous surgery for idiopathic macular holes: results of a pilot study. *Arch Ophthalmol* 1960; 109: 654–659.
- Tranos PG, Ghazi-Nouri SMS, Rubin GS, *et al.* Visual function and subjective perception of visual ability after macular hole surgery. *Am J Ophthalmol* 2004; 138: 995–1002.
- Meng Q, Zhang S, Ling Y, *et al.* Long-term anatomic and visual outcomes of initially closed macular holes. *Am J Ophthalmol* 2011; 151: 896–900.e2.
- Christensen UC, Kroyer K, Sander B, *et al.* Prognostic significance of delayed structural recovery after macular hole surgery. *Ophthalmology* 2009; 116: 2430–2436.
- Baba T, Yamamoto S, Arai M, *et al.* Correlation of visual recovery and presence of photoreceptor inner/outer segment junction in optical coherence images after successful macular hole repair. *Retina* 2008; 28: 453–458.
- Chang LK, Koizumi H and Spaide RF. Disruption of the photoreceptor inner segment-outer segment junction in eyes with macular holes. *Retina* 2008; 28: 969–975.
- Bottoni F, DeAngelis S, Luccarelli S, *et al.* The dynamic healing process of idiopathic macular holes after surgical repair: a spectral-domain optical coherence tomography study. *Invest Ophthalmol Vis Sci* 2011; 52: 4439–4446.
- Roorda A, Romero-Borja F, Iii WJD, *et al.* Adaptive optics scanning laser ophthalmoscopy. *Opt Express* 2002; 10: 405–412.
- Liang J, Williams DR and Miller DT. Supernormal vision and high-resolution retinal imaging through adaptive optics. *J Opt Soc Am A Opt Image Sci Vis* 1997; 14: 2884–2892.
- Viard C, Nakashima K, Lamory B, *et al.* Imaging microscopic structures in pathological retinas using a flood-illumination adaptive optics retinal camera. In: Proceedings of the ophthalmic technologies XXI, San Francisco, CA, 11 February 2011. International Society for Optics and Photonics, <https://www.spiedigitallibrary.org/conference-proceedings-of-spie/7885/788509/Imaging-microscopic-structures-in-pathological-retinas-using-a-flood-illumination/10.1117/12.874766.short>
- De Berg M, Cheong O and Van Kreveld M. *Computational geometry: algorithms and applications*. New York: Springer, <https://www.springer.com/in/book/9783540779735>
- Li KY, Tiruveedhula P and Roorda A. Intersubject variability of foveal cone photoreceptor density in relation to eye length. *Invest Ophthalmol Vis Sci* 2010; 51: 6858–6867.
- Ooto S, Hangai M, Takayama K, *et al.* Photoreceptor damage and foveal sensitivity in surgically closed macular holes: an adaptive optics scanning laser ophthalmoscopy study. *Am J Ophthalmol* 2012; 154: 174–186.e2.
- Gass JDM. Idiopathic senile macular hole: its early stages and pathogenesis. *Arch Ophthalmol* 1988; 106: 629–639.
- Ezra E, Fariss RN, Possin DE, *et al.* Immunocytochemical characterization of macular hole opercula. *Arch Ophthalmol* 2001; 119: 223–231.
- Hansen S, Batson S, Weinlander KM, *et al.* Assessing photoreceptor structure after macular hole closure. *Retin Cases Brief Rep* 2015; 9: 15–20.